Numerical Analysis of Geometry and Hole Effects on Fatigue Crack Growth and Component Lifespan

Erfan Kakavand[1], Amirhossein Parsania[2] and Seyyed Amirhosein Hosseini[3,*]

[1] Department of Mechanical Engineering, Bu-Ali Sina University, Hamedan, 65178-38695, Iran

[2] Department of Mechanical Engineering, Islamic Azad University, Qazvin, 34199-15195, Iran

[3] Department of Industrial, Mechanical and Aerospace Engineering, Buein Zahra Technical University, Buein Zahra, 34517-45346, Qazvin, Iran

INFORMATION

Keywords:
Fatigue crack growth

DOI: 10.23967/j.rimni.2025.10.65831

SCIPEDIA
Revista Internacional de Métodos Numéricos para Cálculo y Diseño en Ingeniería
Revista Internacional Métodos numéricos para cálculo y diseño en ingeniería
RIMNI
In cooperation with CIMNE

Numerical Analysis of Geometry and Hole Effects on Fatigue Crack Growth and Component Lifespan

Erfan Kakavand[1], Amirhossein Parsania[2] and Seyyed Amirhosein Hosseini[3,*]

[1]Department of Mechanical Engineering, Bu-Ali Sina University, Hamedan, 65178-38695, Iran

[2]Department of Mechanical Engineering, Islamic Azad University, Qazvin, 34199-15195, Iran

[3]Department of Industrial, Mechanical and Aerospace Engineering, Buein Zahra Technical University, Buein Zahra, 34517-45346, Qazvin, Iran

ABSTRACT

Mechanical failures have caused significant damage and financial losses. However, compared to the vast number of successful designs for mechanical components and structures, mechanical failures are relatively rare. Mechanical failures involve a highly complex interaction between time, load, and the environment, with the environment comprising two factors: temperature and corrosion. The load can be uniform, steady, variable, uniaxial, or multiaxial. Undesirable effects of cyclic loads lead to crack initiation and growth, ultimately resulting in component failure. In this study, the focus is on increasing the life of components under cyclic loading by investigating crack behavior and development in the presence of stop holes. The investigation was conducted on aluminum 7075. Initially, the arrangement of circular holes in the standard CT sample was obtained using Design Expert software to assess this effect. By performing simulations in Abaqus software, the life of each sample was determined. In the next stage, based on these results, the samples are subjected to examination in the presence of key-shaped notches.

OPEN ACCESS

Received: 22/03/2025

Accepted: 27/05/2025

Published: 27/11/2025

DOI
10.23967/j.rimni.2025.10.65831

Keywords:
Fatigue crack growth

1 Introduction

Fatigue is a material behavior that occurs under cyclic stress or strain, distinct from static loading. Additionally, it is a phenomenon characterized by localized, durable, and gradual deformation of materials where cyclic stress and strain occur at one or multiple points. As cyclic loads are applied, this process leads to the formation of cracks that propagate until they reach their maximum extent. Eventually, after a certain number of cycles, the component fails [1].

By introducing cracks during cyclic loading, components eventually fail after undergoing a certain number of loading cycles. To increase the fatigue life of components, various methods can be employed, including repair and destructive methods. In repair methods, using reinforcing materials to strengthen the component leads to an increased life. In destructive methods, creating permanent deformation and altering stress gradients in the component results in an increased life.

*Correspondence: Seyyed Amirhosein Hosseini (hosseini@bzte.ac.ir).

Song and Shieh [2] researched the use of stop holes to enhance fatigue life. Their study focused on improving crack initiation life and overall fatigue life on aluminum 6061-T651 and stainless steel AISI 304. The experiments were performed on CT specimens, and a stop hole was introduced in front of the initial crack during the fatigue crack growth process. The researchers concluded that the stop hole method eliminates the stress singularity at the crack tip, leading to an increase in the specimen's life due to reduced stress concentration.

Hu et al. [3] investigated the reduction of stress intensity factor and increased fatigue life by introducing stop holes around a crack subjected to cyclic tensile loading. In this research, the size and location of the stop holes were considered variable parameters. Hu found that the position of the stop holes significantly affects the crack rotation angle and remaining fatigue life, emphasizing the importance of reasonable hole drilling. Additionally, both vertical and horizontal distances around the crack play a crucial role in achieving increased fatigue life. Larger hole sizes also contribute to a longer fatigue life, with the most significant changes occurring at 90 and 270 degrees in the circumferential direction.

Razavi et al. [4] studied a novel method called the stop-hole technique to enhance the fatigue life of a cracked component under cyclic tensile loading. A parametric study on various geometric parameters of the double stop-hole was performed. Microscopic investigations alongside numerical results showed that the increase in fatigue life resulting from the double stop-hole technique is notably superior to the conventional single-hole method. Furthermore, the lower stress level around the double stop-hole significantly contributes to the increased fatigue life.

Rahimi et al. [5] conducted simulations and studied the effects of stop holes with different geometries on crack dynamics in brittle materials concerning internal fracture toughness using the ordinary state-based (OSB) aerodynamic method. With the help of OSB analysis, a new, easy-to-use technique was proposed to enhance the crack resistance in materials. Various combinations of double, parabolic, branched, double-parabolic, and mixed parabolic stop holes under tensile loading and T-shaped, I-shaped, double linear, linear, and parabolic linear stop holes under shear loading were suggested in a tabular form and are compared in terms of scientific and applicability. Overall, the proposed geometries were found to be highly effective in enhancing material toughness.

Maleki et al. [6] investigated the influence of the position of a screw in the crack extension direction on mixed-mode fracture strength and the effects of geometry and loading on stress intensity factors through experimental and numerical research. Experimental tests were performed on edge-cracked specimens with screws at different distances from the crack tip, as well as simple (without screw) specimens. Finite element simulations were used to calculate the stress intensity factors. The numerical simulations helped analyze and understand the stress distribution near the crack tip under various loading conditions and screw positions. The results showed that specimens with screws located near the crack tip exhibited significantly increased fracture resistance. Moreover, the geometry of stress intensity factors, indicative of stress concentration at the crack tip, decreased in specimens with screws near the crack tip. This research is valuable for studying the effect of screw position on fracture behavior and stress distribution in structures with cracks. The findings demonstrate that placing a screw near the crack tip can enhance overall resistance and reduce stress concentration, contributing to improved structural integrity.

Chen et al. [7] investigated the fatigue behavior of steel plates with central cracks repaired using CFRP materials. The applied load angles were 0°, 15° and 30° through a specialized loading system. The experimental results of mixed-mode I and II fatigue tests were presented and compared. The fatigue cracks Growth, path, and failure mode were studied to evaluate the effects of CFRP repair,

load angle, and initial crack length. The results showed that the influence of CFRP repair decreases with increasing load angle, while the effect of repair on increasing crack length increases. This study contributes to the current research status on the fatigue behavior of repaired metallic structures under mixed-mode fatigue loading.

Pavlou [8] investigated the delayed fatigue crack Growth in mixed-mode cracks with stop-holes. An aluminum Al-2024 plate was subjected to mechanical loading in this research. Parameters of varying crack inclination angles and stop-hole diameters were examined, and the results showed that the fatigue crack Growth rate for mixed-mode cracks is lower for cracks with smaller inclination angles. Larger stop-holes lead to a better increase in fatigue life compared to smaller stop-holes.

Masoudi Nejad et al. [9] conducted a study on predicting fatigue crack Growth and fractography in steel rails. They used both numerical and experimental methods to investigate the behavior of fatigue crack Growth in this type of steel. First, fatigue crack Growth tests and hardness tests were performed, and then the results were examined by studying fractography on the fractured specimens. Hardness measurements were taken at different points on the specimens. Subsequently, three-dimensional finite element analysis was utilized to study the fatigue crack Growth under stress fields. The modified Paris model was employed to predict the fatigue crack Growth rate. Finally, the results of the three-dimensional finite element analysis were found to be in good agreement with the experimental results.

Alshoaibi [10] conducted a computational simulation of three-dimensional fatigue crack Growth under mixed-mode loading and investigated the influence of hole presence and geometrical thickness on fatigue crack Growth and fatigue life under constant amplitude loading. The study involved mixed-mode (I/II) fatigue crack Growth on a plate with three holes and various thicknesses, as well as on a CTS specimen with different thicknesses and loading angles. Geometrical thickness had no significant effect on the crack path, but changes in specimen thickness had a considerable impact on stress and strain distributions. The stress-strain field near the crack tip shifted from plane stress to plane strain with increasing specimen thickness, indicating three-dimensional stress on the crack tip and confinement of the plastic zone within a small domain. Similarly, with increased geometrical thickness, the equivalent Von Mises stress and maximum principal stress decreased at a nearly proportional rate equal to the thickness increment. As predicted, fatigue cracks propagated toward the holes in these simulation sequences, where the holes acted as barriers to crack growth and attracted the crack path.

Gong et al. [11] presented an improved model capable of predicting fatigue crack growth under variable amplitude loading. The model combines the effects of crack closure and residual stresses. The phenomenon of overload acceleration and the delay in crack growth rate reduction, considering the changes in stress due to crack closure, are taken into account. The predicted growth rates for fatigue crack growth have been validated with experimental data from several steels and alloys. The fatigue life prediction of the model has also been confirmed through Monte Carlo simulations. The simulation errors in different loading sequences are less than 10%. This study can be used for the fatigue design of metal structures.

Liao et al. [12] investigated the effect of the size and relative position of a hole on the crack deflection angle in a repaired structure. By comparing the computational and experimental results, they observed that changes in the hole radius, vertical distance of the hole, and horizontal distance of the hole in the repaired structure have various effects on the crack growth path. When the hole radius is 2 mm (approximately 2% relative hole radius), the vertical distance of the hole is 4 mm (approximately 4% relative vertical distance), and the horizontal distance of the hole is 14 mm (approximately 16% relative horizontal distance), the stress intensity factor is higher, the edge stress along the crack growth path has a stronger “attracting” effect, and the crack deflection angle is larger. From the computational

results, optimal dimensions and positions of the adhesive and hole can deflect the crack to a larger angle and simultaneously extend the life of the structure.

Shi et al. [13] conducted a study on the ultimate strength of a crack-damaged stiffened panel repaired using Carbon Fibre Reinforced Polymer (CFRP) and stop-hole technique, utilizing both numerical and experimental methods. Initially, a crack was present in the panel, and then it was repaired using CFRP and a stop-hole technique. The ultimate strength of the repaired panel was examined through experiments and numerical analyses. The results showed that the use of CFRP and the stop-hole technique can significantly improve the ultimate strength of the cracked stiffened panel.

Kakavand et al. [14] investigated fatigue crack Growth in aluminum 7075T6 specimens under mechanical and thermal loading. They performed fatigue tests on CT specimens at temperatures of 27, 110, and 190 degrees Celsius and found that the fatigue life of the specimens decreases at higher temperatures. In the next stage, the specimens were tested under combined mechanical and thermal loading. During these tests, the specimens were subjected to mechanical loading with a variable frequency, and it was observed that the N coefficient in the Paris equation remained constant. They were also able to determine variations in the C coefficient in the Paris equation with respect to the loading frequency.

Deng et al. [15] conducted a study on predicting fatigue crack growth using stress-controlled central crack fatigue tests with stop-holes. The results indicate that stop-holes change the crack growth path and lead to the initiation of secondary cracks from the bottom edge of the stop-hole. The increase in fatigue life is mainly attributed to the occurrence of secondary cracks. Additionally, it is observed that larger stop-hole radii result in longer fatigue life.

Fang et al. [16] investigated the effect of bolt reinforcement in a plate containing a fatigue crack and stop-holes, subjected to out-of-plane bending loads. Bolt reinforcement can significantly control the in-plane compression and out-of-plane shear deformation and reduce the accumulation of fatigue damage near the crack tip, inhibiting its continuous growth. The effect of dual-bolt reinforcement is considerable and does not create additional local stiffness to induce new fatigue cracks. Excessive tightening force does not improve reinforcement and may even increase the risk of crack initiation at the bolt edge, while an appropriate ratio of load to tightening force is around 3:1. The fatigue life of components is negatively linearly related to the nominal stress in the bolt, allowing for quantitative prediction of fatigue life.

Gong et al. [17] investigated the effect of stop-holes on the path and fatigue life of mixed-mode I-II fatigue cracks under combined rotational loading. Specimens with different stop-hole diameters were used in tension and shear loading under various loading angles. The results showed that the fatigue life increases directly with the loading angle and stop-hole diameter. Numerical simulations were used to enhance the experimental database. Based on this database, a recurrent neural network with variable lengths was proposed to retain crack information from the previous learning stage. The results are promising and inspire evaluating component safety.

Anoop Kumar et al. [18] investigated the effect of different hole shapes (circular, square, and elliptical) located near a central crack in a finite plate under tensile loading. The objective was to examine the effectiveness of these holes in arresting crack growth when introduced parallel and perpendicular to the central crack axis. The investigation was carried out using numerical simulations, where a two-dimensional model of the finite plate with a central crack was created and validated against analytical results. Then, the holes were systematically introduced to analyze their influence on the stress intensity factor for mode I conditions.

Neto et al. [19] studied the influence of two symmetrical holes next to a crack and its effect on the fatigue crack growth rate (FCG) using numerical methods. The FCG rate increases (decreases) when the crack tip is behind the holes, and this behavior is amplified with an increase in hole diameter and a decrease in their spacing. This effect is attributed to changes in the size of the plastic zone. The experimental work confirmed the findings of the numerical model and demonstrated that cumulative plastic strain at the crack tip is a significant driving force for crack growth, and cyclic plastic deformation is the main mechanism of FCG damage.

Baptista et al. [20] analyzed fatigue crack growth under mixed conditions using artificial neural networks. Mixed conditions were achieved by combining a flexible specimen with four flexure points at different shear positions and a compressive stress specimen. To train artificial neural networks, the crack tip displacement vector distribution criterion was used in the simulations. After complete training, the neural networks were capable of predicting crack paths and fatigue crack growth life under mixed conditions and showed good agreement with experimental and numerical samples.

Liu et al. [21] conducted a study on the "drilling stop hole" method and the use of Fiber-Reinforced Polymer (FRP) for repairing cracked steel plates under cyclic loading. The initiation and growth of cracks were examined through experimental tests. The stress distribution in the stop hole and the remaining fatigue life were evaluated using the Finite Element Method. The impact of prolonging the remaining fatigue life was analyzed. The results indicated that the effectiveness of using only stop holes is limited, whereas the combination of the "drilling stop hole" method and FRP reinforcement significantly extended the remaining fatigue life. This effect is mostly dependent on the increase in the crack initiation life from the stop hole.

Feng et al. [22] analyzed the parameters of stop holes for fatigue cracks on the edge of the arches in a steel bridge's roof. Two types of fatigue cracks on the arches were repaired using stop holes. The effect of stop holes with different diameters and positions was investigated. Based on Finite Element Models, the variations in stress distribution and stress combination effects for different stop hole diameters and position were compared. The analysis results showed that stop holes can effectively improve stress concentration near the crack edge and significantly increase the fatigue life of the components. The performance of crack arrest improves with the increase in stop hole diameter, but large stop holes may not effectively slow down crack growth. Stop holes located at $-0.5D$ to $0.5D$ from the crack edge exhibit good performance. If the stop hole is located either outside or inside the crack, the point of maximum stress still appears at the crack edge. The diameter of the stop hole does not have a significant effect on its location. Parsania et al. [23] analyze the interaction between parallel adjacent cracks in an infinite plate under tensile and compressive stresses using Abaqus and the J-integral method. Results show that adjacent cracks can intensify, protect, or have no effect depending on their distance and angle. A neural network (MLP) was also used to predict the secondary crack's influence. Zhang and Wei [24] introduce the ANN-L method, combining artificial neural networks with Lagrange interpolation to improve fatigue crack growth (FCG) life predictions under variable amplitude loading. Results show ANN-L outperforms traditional models and other ANN approaches, especially in overload retardation intervals. The method demonstrates excellent accuracy and potential for enhancing fatigue life prediction in structural materials.

In this study, the behavior of crack propagation and growth in the presence of stop holes was investigated. The research was conducted on 7075 aluminum alloys. Initially, to examine this effect, the Design Expert software was used to determine the optimal arrangement of circular holes on a standard CT (Compact Tension) specimen. Simulations were then carried out using Abaqus software to evaluate

the fatigue life of each specimen. In the next stage, based on these results, specimens featuring elliptical (bean-shaped) notches were analyzed.

According to Fig. 1, the stress intensity factor converges with a mesh size of 0.05 mm, and this size is used for simulation in this article as well. Table 1 compares the values obtained from the software with the analytically calculated values, showing that the simulation is performed with a maximum error percentage of 1.48%.

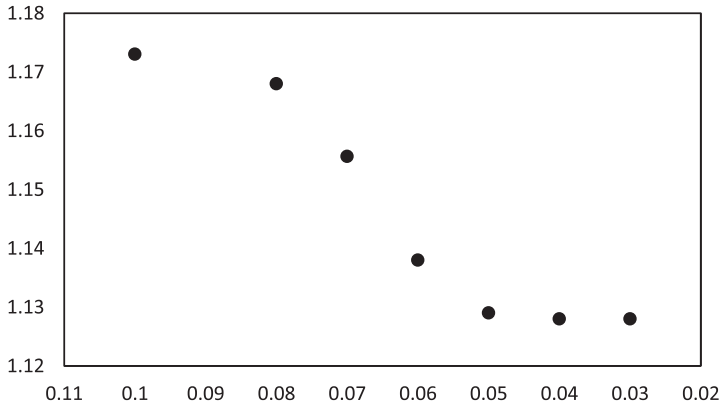

Figure 1: Converging stress intensity factor

Table 1: Stress intensity factor for a singular crack in different angles and modes

Mode	First mode				Second mode	
Angle	0	15	30	45	15	30
Software	1.13×10^6	1.03×10^6	8.53×10^5	5.66×10^5	2.84×10^5	4.93×10^5
Theory	1.12×10^6	1.05×10^6	8.41×10^5	5.60×10^5	2.80×10^5	4.85×10^5
e%	1.01	1.27	1.46	1.02	1.18	1.48

2 Crack Modeling

In this study, crack growth modelling is performed using the well-known Paris and Erdogan power law equation [25], commonly known as the Paris equation. This equation is used to the first application of fracture mechanics and is represented as follows:

$$\frac{\mathrm{d}a}{\mathrm{d}N} = C_p(\Delta K)^{mp} \tag{1}$$

where C_P is the width and m_P is the slope of the $\log \Delta K - \log \mathrm{d}a/\mathrm{d}N$ curve.

To simulate fatigue crack growth, the initial crack is first propagated in very small increments. Then, using the Abaqus software, the stress intensity factors for mode I and mode II are calculated. Then, using the maximum stresses ($\Delta\sigma\theta_{max}$). The effective stress intensity factor in mode I and mode II is calculated as follows:

$$\Delta K_{eff} = \Delta K_I cos^3\left(\frac{\theta_c}{2}\right) - 3\Delta K_{II} cos^2\left(\frac{\theta_c}{2}\right) sin\left(\frac{\theta_c}{2}\right) \tag{2}$$

The change in crack length ($\Delta a/\Delta N$) is then obtained from the assumption of constant stress intensity factor changes along small cracks, using Eq. (1). Additionally, for predicting the crack initiation life, the Manson-Coffin equation is used [25]:

$$\frac{\Delta\varepsilon}{2} = \frac{\sigma_f^{'}}{E}(2N_f)^b + \varepsilon_f^{'}(2N_f)^c \tag{3}$$

The simulations are carried out using the ABAQUS software, and due to the thickness of the specimen, plane strain analysis is used. Eventually, for meshing crack-containing samples in the software, the element of the 8-node quadrilateral, plane strain, reduced integration, and fourth-order, known as CPE8R in the software, is chosen. In finite element analyses, the size of elements significantly affects the obtained results. Investigating the effect of element size on convergence is one of the essential considerations for any finite element analysis. Considering the results, the dimensions of the elements around the crack tip is set to be 300 μm. Fig. 2 illustrates the meshing of the crack tip.

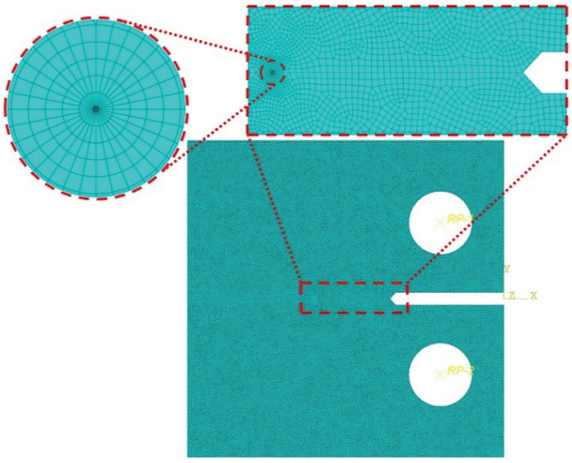

Figure 2: Crack-tip meshing

The crack growth simulations are performed on aluminum 7075-T6 specimens under cyclic tension loading with a maximum load of 10 kN and a minimum load of zero. The mechanical properties of 7075-T6 aluminum alloy are presented in Table 2 and the loading conditions are illustrated in Fig. 3.

Table 2: Mechanical properties of AL 7075-T6

σ_y (MPa)	σ_u (MPa)	E (GPa)	v	K_{Ic} $(MPa\sqrt{m})$
496	572	71.6	0.33	29

The initial simulations involved creating holes in the specimen at specific horizontal (H) and vertical (V) distances and with a diameter (D) of the hole. Fig. 4 illustrates the positions of the holes at each stage of the simulation. As illustrated in Fig. 4, five different configurations of horizontal and vertical spacing were analyzed for each of the three hole diameters (2, 4, and 6 mm). Following the proposed software's DOE pattern, the holes were placed at the vertices of a square and the center of a circle. In each specimen, a hole was drilled at the specified position, and the loading was applied to it. For example, the index H6/V3 represents a hole positioned 6 mm horizontally and 3 mm vertically.

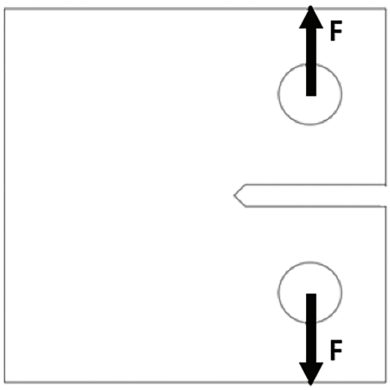

Figure 3: The way of samples' loading

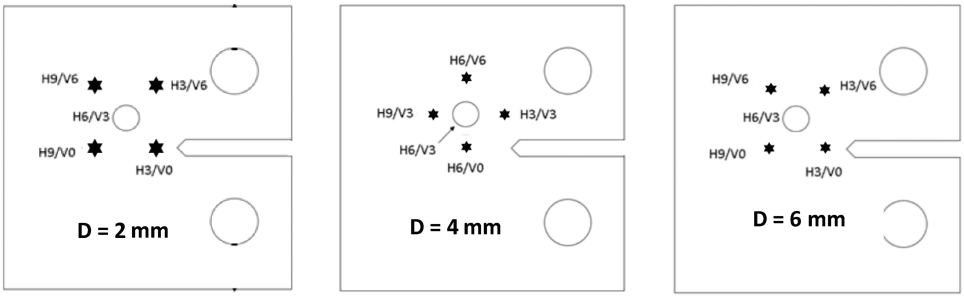

Figure 4: Positions of the holes. (**a**) D = 2 mm; (**b**) D = 4 mm; (**c**) D = 6 mm

2.1 The Simulations of the Specimens with Circular Holes

Fig. 5 depicts the lifetimes of the specimens containing holes at specific distances. The lifetime of the specimens is divided into three parts. The first part represents the initial crack growth from the notch to the hole, denoted as N_1. After the crack reaches the hole, the crack growth is arrested until the first crack initiation occurs at the hole's periphery after several loading cycles, denoted as N_2. The third part represents the lifetime after the crack initiates from the hole, leading to the complete failure of the specimen, denoted as N_3. For the first part of crack growth (N_1 and N_3). The lifetime estimation was carried out using the Paris equation. For the second part of the lifetime (N_2), the lifetime estimation was performed using the Manson-Coffin equation.

In the first stage of crack growth, as seen in Figs. 6 and 7. The three cases of H9/V6, H3/V6, and H6/V3 exhibit approximately similar lifetimes. The reason for this is that the hole is far enough from the initial crack, and its influence on the crack is minimal. However, these holes do contribute to an increase in the lifetime of the specimens, but the crack does not propagate into the holes; it merely deviates from its original path. This deviation occurs because creating holes in the specimen causes the loading and stress conditions on the crack tip to no longer be symmetric, leading the crack to transition from Mode I to a combination of Mode I and Mode II. Consequently, the crack does not follow a direct path.

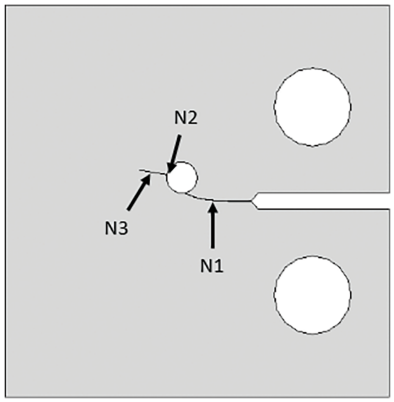

Figure 5: The crack growth steps of a sample

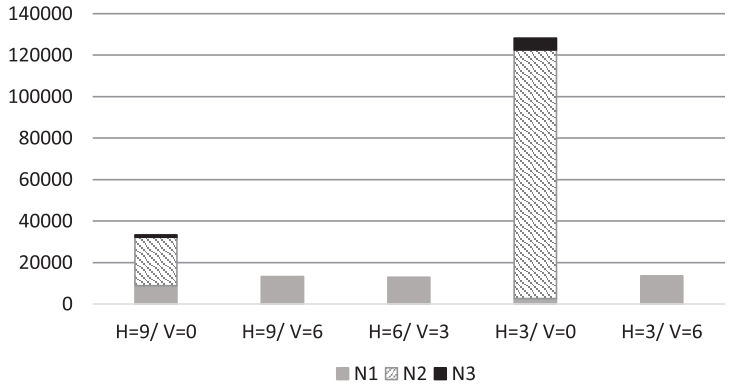

Figure 6: Total lifetime of the specimens with a 2-mm hole diameter

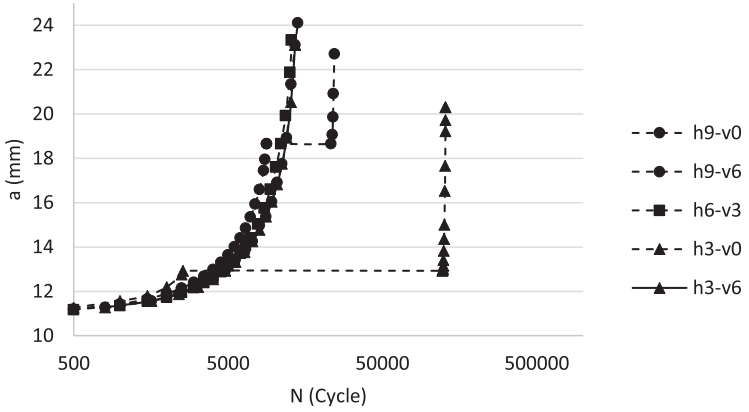

Figure 7: a-Nf sample figure with a 2-mm hole diameter

In the cases of H9/V0 and H3/V0, as depicted in Fig. 6: The crack has entered its second and third stages of growth. Therefore, in the H3/V0 case, the hole is very close to the crack, and as a result, the crack quickly reaches the hole, leading to a shorter initial lifetime. However, in this case, the second stage of crack growth or crack initiation lifetime is longer compared to the H9/V0 case because the

strains induced around the hole are lower. Additionally, the third stage of crack growth is also longer in this case because after its initiation, the crack has a longer path to propagate before reaching its critical length.

In Fig. 8, it can be observed that H6/V0 and H3/V3 cases have the lowest initial fatigue life. This is because the holes are closer to the crack tip in these cases, causing the cracks to quickly reach the holes.

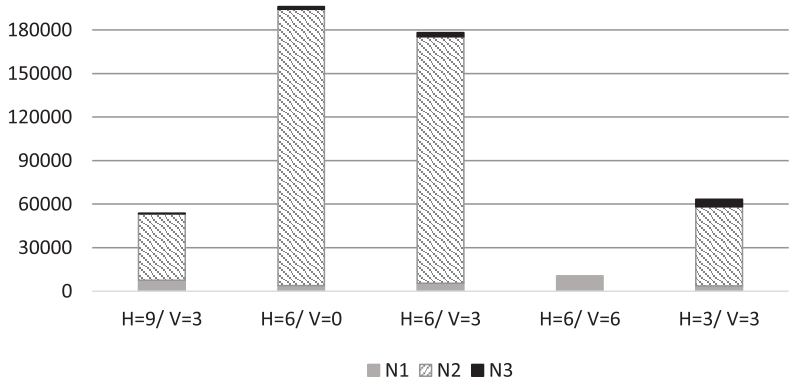

Figure 8: Total lifetime of the specimens with a 4-mm hole diameter

By comparing the two H9/V3 and H6/V3 cases in Fig. 8, the specimen with H9/V3 has a longer fatigue life. This is because the crack follows a longer path to reach the hole. In the H6/V6 case, the crack does not reach the hole and continues to propagate to its critical length. In H9/V3, a part of the reduction in fatigue life due to the hole is compensated by the longer crack path to the hole during the first stage. However, in the third stage, the shorter crack length and higher stress intensity factor in H9/V3 result in a shorter fatigue life compared to the other cases.

In the cases of H6/V0 and H6/V3, as shown in Fig. 9, it can be observed that H6/V0 has a longer fatigue life. This is due to the symmetry of loading in the specimen, which preserves the life in mode I. This also affects the third stage, resulting in a longer life compared to the other cases. In Fig. 10, the crack growth path for the specimen under condition H3/V3 for D = 4 mm is shown. Additionally, the stress distribution contour for this case is provided in the same figure.

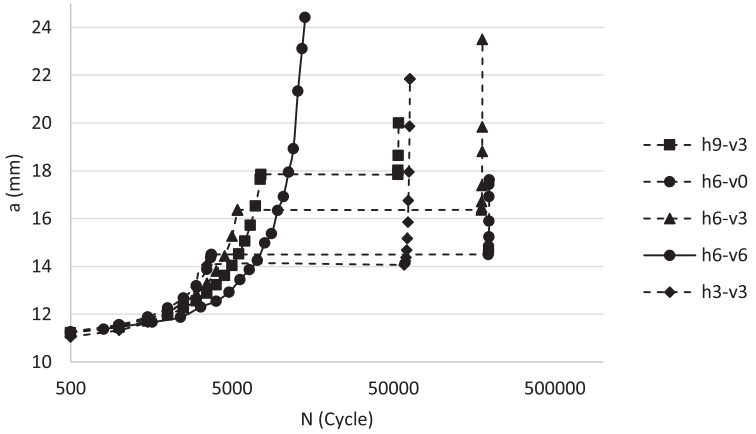

Figure 9: a-Nf sample figure with a 4-mm hole diameter

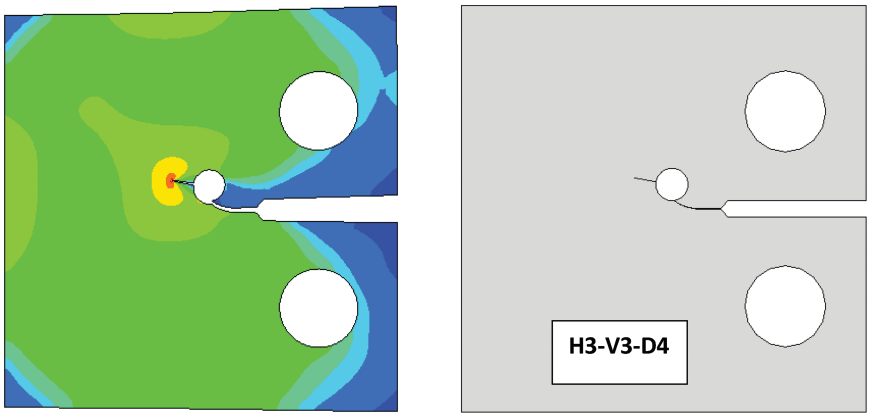

Figure 10: Stress contour and path of crack growth of samples with a hole diameter of 4 mm

For the specimens with a 6-mm hole diameter in the H3/V0 case, as seen in Fig. 11. The hole is precisely located at the crack tip, and thus, there is no initial fatigue life. In the H9/V6 case, although the hole is far from the crack, the crack still reaches the hole faster due to the larger hole diameter, which significantly influences the stress at the crack tip and accelerates the crack to mode I and mode II growth. The same effect can be observed in H3/V6 and H6/V3. The increase in diameter has a considerable impact on the crack behavior due to its effect on the stress concentration around the hole. In the H9/V0 case (Fig. 12), the crack remains in mode I due to the geometric symmetry until it reaches the stop hole. In the H9/V6 case, the crack follows a longer path before reaching the stop hole. However, due to the significant distance between the stop hole and the applied load, more severe stress concentration is observed around the stop hole. As a result, the fatigue life in the second stage is reduced compared to other configurations. This observation is also applicable to the H9/V0 case, where the symmetry of loading results in a longer fatigue life in the second stage compared to the previous case. By comparing this case with a similar one with a 2 mm hole, it can be concluded that the diameter has a significant impact on increasing the fatigue life in the second stage and reducing it in the first stage. In the H3/V0 and H3/V6 cases, a substantial increase in fatigue life is observed compared to the 2 mm hole diameter, which is due to the reduction in stress concentration resulting from the larger hole diameter. Regarding the results of the third-stage fatigue life, it can be observed that the fatigue life in the H9/V0, H9/V6, and H6/V3 cases is lower compared to the other two cases. This is because the stop hole is farther away from the crack tip, leading to quicker reaching of the critical crack length. By examining the total life curve for the 6-mm hole diameter, it can be concluded that the second stage of life has a significant effect, to the extent that the effect of the first and third stages is not visible in the curve for H3/V0 and H3/V6 cases.

After obtaining the simulation results, the lifetime values of the samples were fed into the Design of Expert software. This software models the data based on a central composite algorithm and optimizes it accordingly. The values A, B, and C correspond to H, V, and d, respectively (Table 3).

Based on the simulation results, it can be concluded that the hole should be created at the nearest point to the crack to increase the specimen's lifetime. Observing the lifetime diagrams also reveals that a larger hole diameter leads to better results, but the exact optimal diameter is not explicitly determined. Therefore, additional simulations were conducted for various horizontal and vertical distances to find the suitable diameter, as shown in Fig. 13.

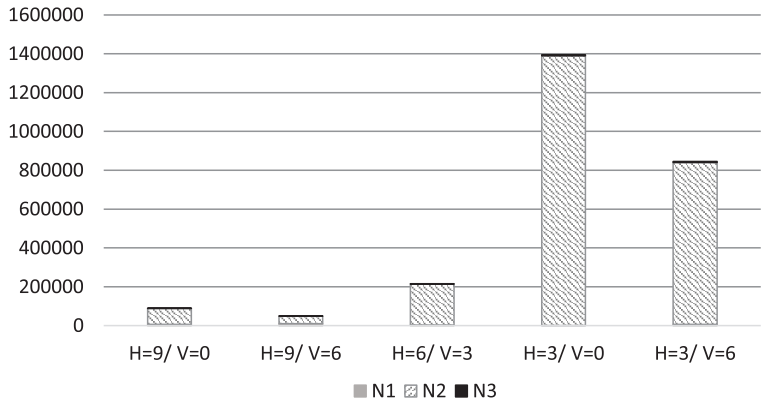

Figure 11: Total lifetime of the specimens with a 6-mm hole diameter

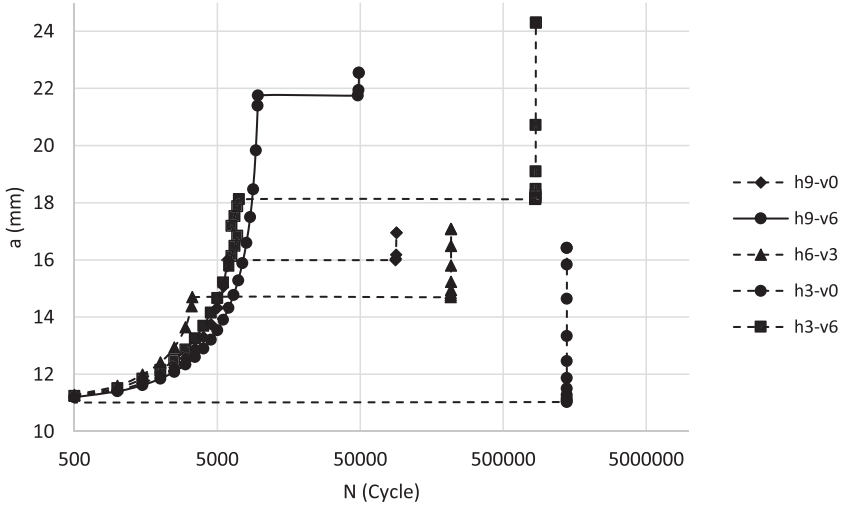

Figure 12: a-Nf sample figure with a 4-mm hole dimeter

Table 3: Design expert software predication for maximizing the lifetime

Factor	Name	Level	Low level	High level	Std. Dev.	Coding
A	A	1	−1	1	0	Actual
B	B	−1	−1	1	0	Actual
C	C	1	−1	1	0	Actual
Response	Prediction					
R1	994,518					

It can be observed from Fig. 13. Starting from a diameter of 9.5 mm, the lifetime decreases. This decrease is attributed to an increased concentration of stress around the hole, resulting in higher stress and strain, consequently leading to a reduced lifetime.

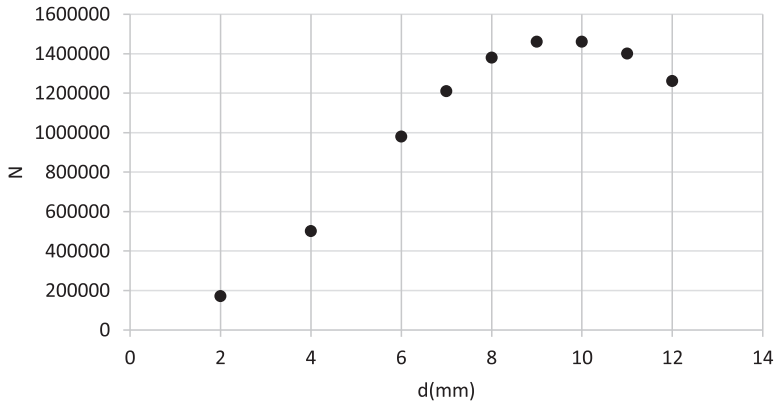

Figure 13: The impact of the hole diameter on the specimen's lifetime at H0–V0 distance

2.2 Simulation of Specimens with a Slotted Hole

Based on the results obtained from the circular hole simulations, it can be concluded that the closer the hole is to the crack, the longer the lifetime of the specimens. Therefore, to reduce the analysis steps, the results from the circular hole simulations were used, and for the slotted hole configuration, the shape of the slot was created at the crack tip, and three parameters (length, diameter, and angle of placement of the slotted holes) were examined, and the lifetime of the specimens was analyzed (Fig. 14).

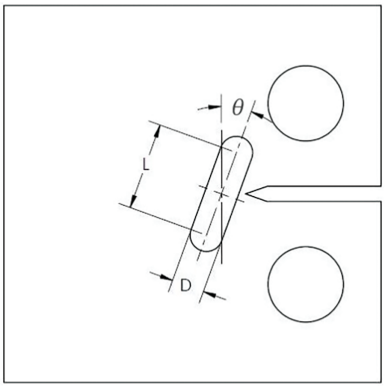

Figure 14: Schematic of the slotted holes

The diagrams were examined for cases with a constant angle, and since the slots were created immediately after the crack tip, the total lifetime of the specimens was divided into two parts, similar to the previous stage. The initial lifetime was excluded, and the total lifetime was divided into the sum of the first part for creating the crack at the edge of the slot and the second part for the crack growth until the specimens failed.

In the design and experimentation of these simulations, similar to the circular hole cases, the range of slot length was set from zero to 10 mm, the range of slot diameter was set from 2 to 6 mm, and the angle was divided into intervals from zero to 60 degrees.

For a better understanding of the parameter's effects in the 2D representation, the diagrams of the specimens were examined for a constant angle. In the case of d = 2 and two lengths (l = 0 and

l = 10), as shown in Fig. 15, it can be observed that as the length increases, there is a slight increase in the approximate total lifetime, which could be attributed to the reduced stress concentration around the slot. This finding suggests that there might be a specific slot length in which the specimen's lifetime reaches its maximum value.

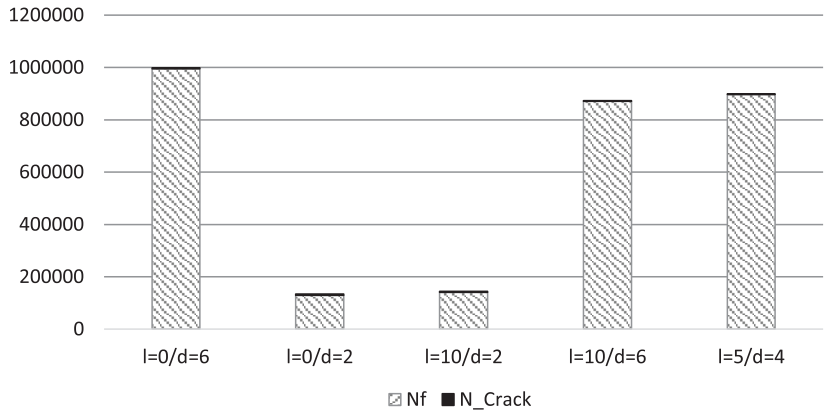

Figure 15: Lifetime diagram of the sample with a 0-degree slot

In the case of d = 6 and two lengths (l = 0 and l = 10), as observed, the increase in the first stage of the lifetime is opposite to the previous case. The reason behind this is the increased stress concentration around the circular part of the slot in comparison to the hole. However, this increased lifetime does not have significant differences.

In the case of l = 5 and d = 4, the total lifetime is almost equal to the case of l = 10 and d = 6. It can be concluded that by reducing the slot length, the effect of decreasing the diameter is diminished. The lifetime of the specimens in the second stage (N_crack2) (in the N3 circular hole case) is small enough to be negligible compared to their initial lifetime (Nf).

In the cases of L = 5, d = 4; l = 10, d = 4; and l = 0, d = 4, as shown in Fig. 16, it is observed that reducing the slot length significantly increases the lifetime of the samples. The reason behind this is that the slot is at an angle, and as the length increases, the stress deviates from the symmetric state, creating a mixed-mode condition and consequently increasing stress concentration.

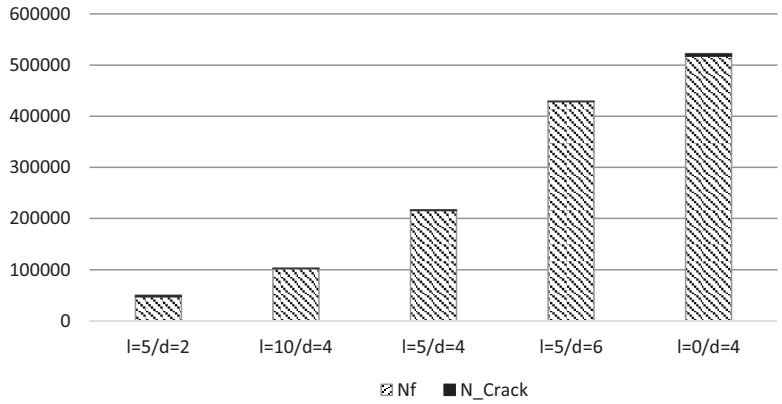

Figure 16: Lifetime diagram of the sample with a 30-degree slot

In the cases of l = 5, d = 6 and l = 5, d = 4, it can also be concluded that increasing the hole diameter leads to an increase in the lifetime. Similarly, in the cases of l = 5, d = 2; l = 5, d = 4; and l = 5, d = 6, increasing the diameter results in a longer lifetime due to the reduction of stress concentration in the samples (Fig. 16).

The lifetime values obtained for the samples (Fig. 17) compared to the lifetime obtained at 0 and 30-degree angles indicate the impact of increasing the angle in reducing the lifetime of the samples. This impact can be observed by comparing two samples, l = 10, d = 6 and l = 0, d = 6, in the lifetime diagram (Fig. 17). Hence, it can be concluded that the angle significantly affects the stress concentration, and as the angle increases, the stress concentration intensifies.

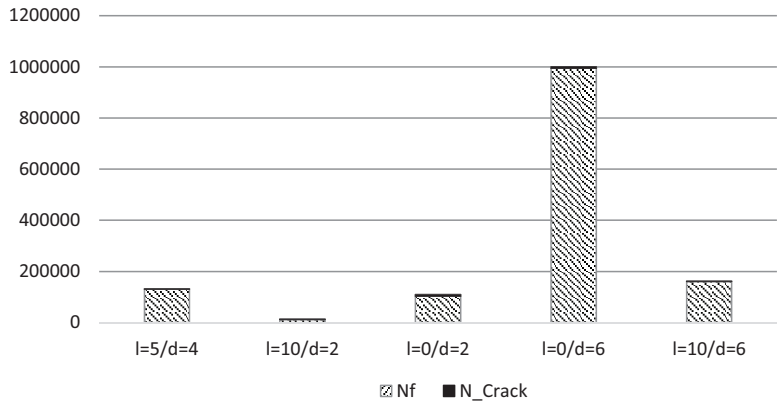

Figure 17: Lifetime diagram of the sample with a 60-degree slot

In the cases of l = 10, d = 2 and l = 0, d = 2, as shown in Fig. 17, increasing the length results in a decrease in the lifetime, while at 0-degree angle, it led to an increase in the lifetime. This observation reaffirms the negative impact of increasing the slot angle on the lifetime increase.

In the investigation of slotted samples, it can be concluded that the change in the slot angle relative to the crack perpendicular has a significant impact. As the angle approaches 90 degrees, the lifetime of the samples decreases. Additionally, the changes in the hole diameter also show that as the diameter approaches 6 mm, the lifetime increases.

The effect of the slot length is observed in only one case, which is at 0-degree angle and for diameter d = 2 mm. Based on the results, the length of 10 mm compared to 0 mm was observed, but it cannot firmly state the influence of the slot length on the lifetime increase. Therefore, once again, the DOE software was utilized to determine whether there are other combinations of diameter, length, and angle that can yield the maximum lifetime (Table 4).

Therefore, at a diameter of 6 mm and a slot angle of 0 degrees, with a length of 2.8 mm, the maximum lifetime was obtained, indicating the significant influence of the slot length on increasing the lifetime.

As it was found that the maximum lifetime occurs at a slot angle of 0 degrees, and previously, for circular holes with a diameter larger than 9.5 mm, the highest lifetime was achieved, further simulations were conducted to find the optimal slot length. The results are presented in Fig. 17.

Fig. 18 illustrates that the lifetime of slotted samples with a diameter of 9.5 mm and a slot length of 2.5 mm is higher than the lifetime of circular holes with the same diameter.

Table 4: Extracted results of parameters and maximum lifetime from the DOE software

Factor	Name	Level	Low level	High level	Std. Dev.	Coding
A	A	−0.44	−1	1	0	Actual
B	B	1	−1	1	0	Actual
C	C	−1	−1	1	0	Actual
Response	Prediction					
R1	1,137,446					

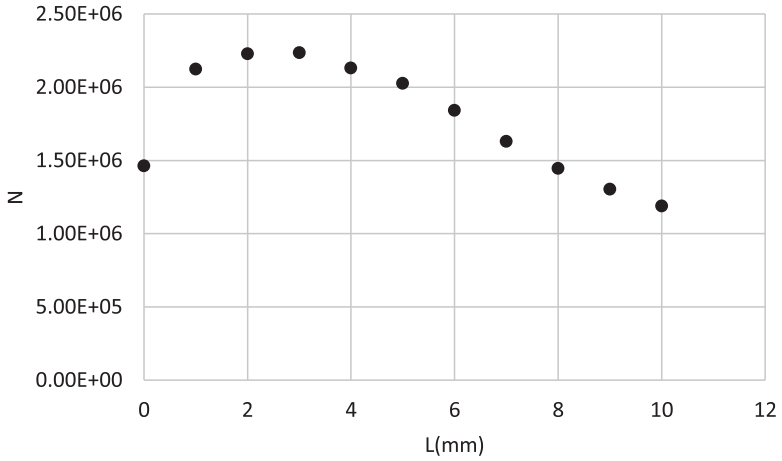

Figure 18: The impact of the slot length on the sample lifetime with a slotted hole of 9.5 mm at a zero-degree angle

To investigate the crack behavior in slotted holes for various diameters and lengths, simulations and calculations of the lifetime were performed, and the results are shown in Fig. 19.

From Fig. 19: The slotted hole with a diameter of 10 mm and a length ranging from 2 to 3 mm exhibits the maximum lifetime among all tested cases. Furthermore, the increase in lifetime due to grooving can be observed in all the plotted curves. However, it can be observed that for a diameter of 12 mm, there is a decrease in lifetime compared to the diameter of 10 mm.

To predict the optimal lifetime, extensive simulations and calculations using the Manson-Coffin relationship are required. Therefore, one of the methods for obtaining the optimal lifetime with multiple input variables is using the DOE approach, which was employed to find the optimal lifetime for a slotted hole with a diameter of 9.5 mm and a length of 2.8 mm.

The lifetime of the circular-shaped hole, specifically the slotted hole with a length of zero, has certain values where the graphs intersect the vertical axis of the lifetime.

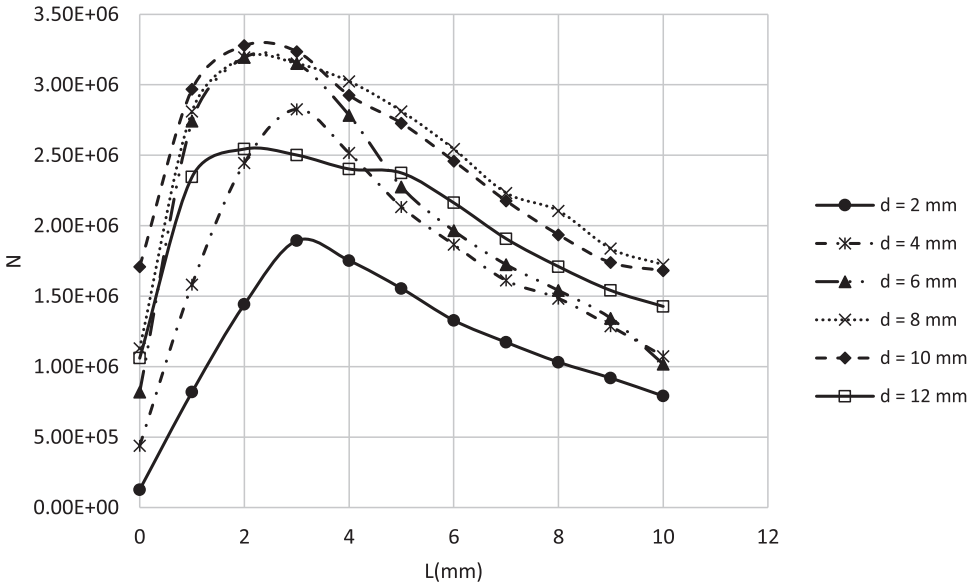

Figure 19: The behavior of the sample lifetime with different diameters and lengths of the slotted holes

3 Conclusion

Based on the conducted simulations involving circular-shaped holes, it was observed that holes located closer to the crack and with larger diameters tend to be more effective. Subsequently, an additional simulation was carried out to determine the optimal hole diameter for enhancing the specimen's fatigue life. For this purpose, holes with diameters ranging from 2 to 12 mm were introduced at the crack tip to assess their effect. It was found that diameters exceeding 9.5 mm lead to a reduction in specimen lifetime, due to increased stress concentrations resulting in higher local stress and strain around the hole.

In the subsequent stage, slotted-shaped holes were created at the crack tip, and their length, diameter, and angle were investigated. The simulations revealed that angled slots decrease the lifetime, while increasing the diameter improves the lifetime. Additionally, it was found that increasing the length of the slot enhances the lifetime. To enable a more accurate comparison between slot length and specimen lifetime, in relation to circular holes, simulations were carried out using a groove diameter of 9.5 mm and slot lengths ranging from 0 to 10 mm. The maximum lifetime was observed at a slot length of 2.5 mm.

The lifetime increase in the case of slotted holes is approximately 53% higher compared to the case of samples with circular holes. However, it should be noted that creating slots in the sample incurs higher costs compared to drilling holes in it.

Acknowledgement: The authors would like to express their sincere appreciation to all individuals and institutions who provided invaluable support and assistance throughout the course of this research.

Funding Statement: The authors received no specific funding for this study.

Author Contributions: The authors confirm contribution to the paper as follows: study conception and design: Erfan Kakavand; data collection: Amirhossein Parsania; analysis and interpretation of

results: Seyyed Amirhosein Hosseini, Erfan Kakavand and Amirhossein Parsania; draft manuscript preparation: Seyyed Amirhosein Hosseini and Amirhossein Parsania. All authors reviewed the results and approved the final version of the manuscript.

Availability of Data and Materials: The data underpinning the findings of this study can be obtained from the corresponding author upon reasonable request.

Ethics Approval: There were no ethical issues involved in this study.

Conflicts of Interest: The authors declare no conflicts of interest to report regarding the present study.

References

1. Stephens RI, Fatemi A, Stephens RR, Fuchs HO. Metal fatigue in engineering. New York, NY, USA: Wiley; 2000.
2. Song PS, Shieh YL. Stop drilling procedure for fatigue life improvement. Int J Fatigue. 2004;26(12):1333–9. doi:10.1016/j.ijfatigue.2004.04.009.
3. Hu Y, Song M, Liu J, Lei M. Effects of stop hole on crack turning, residual fatigue life and crack tip stress field. J Braz Soc Mech Sci Eng. 2020;42(5):216. doi:10.1007/s40430-020-02299-1.
4. Razavi N, Ayatollahi MR, Sommitsch C, Moser C. Retardation of fatigue crack growth in high strength steel S690 using a modified stop-hole technique. Eng Fract Mech. 2017;169:226–37. doi:10.1016/j.engfracmech.2016.11.013.
5. Rahimi MN, Kefal A, Yildiz M, Oterkus E. An ordinary state-based peridynamic model for toughness enhancement of brittle materials through drilling stop-holes. Int J Mech Sci. 2020;182:105773. doi:10.1016/j.ijmecsci.2020.105773.
6. Maleki HN, Abazadeh B, Chakherlou TN. Experimental and numerical investigations of the effect of bolt position on the mixed-mode fracture strength of edge crack specimens. J Aerosp Eng. 2020;33(6):04020078. doi:10.1061/(asce)as.1943-5525.0001192.
7. Chen T, Huang C, Hu L, Song X. Experimental study on mixed-mode fatigue behavior of center cracked steel plates repaired with CFRP materials. Thin-Walled Struct. 2019;135:486–93. doi:10.1016/j.tws.2018.11.030.
8. Pavlou DG. Mode I + II fatigue crack growth delay by stop-holes. J Aerosp Technol Manage. 2018;10:e1518. doi:10.5028/jatm.v10.808.
9. Masoudi Nejad R, Shariati M, Farhangdoost K. Prediction of fatigue crack propagation and fractography of rail steel. Theor Appl Fract Mech. 2019;101:320–31. doi:10.1016/j.tafmec.2019.03.016.
10. Alshoaibi AM. Computational simulation of 3D fatigue crack growth under mixed-mode loading. Appl Sci. 2021;11(13):5953. doi:10.3390/app11135953.
11. Gong H, Yang F-P, Chen T. An improved prediction model on fatigue crack growth rate under variable amplitude loads for metallic materials. J Mater Eng Perform. 2022;31(6):4735–45. doi:10.1007/s11665-021-06562-x.
12. Liao Y, Li Y, Huang M, Wang B, Yang Y, Pei S. Effect of hole relative size and position on crack deflection angle of repaired structure. Theor Appl Fract Mech. 2019;101:92–102. doi:10.1016/j.tafmec.2019.02.010.
13. Shi XH, Hu Z, Zhang J, Guedes Soares C. Ultimate strength of a cracked stiffened panel repaired by CFRP and stop holes. Ocean Eng. 2021;226:108850. doi:10.1016/j.oceaneng.2021.108850.
14. Kakavand E, Seifi R, Abolfathi M. An investigation on the crack growth in aluminum alloy 7075-T6 under cyclic mechanical and thermal loads. Theor Appl Fract Mech. 2022;122:103585. doi:10.1016/j.tafmec.2022.103585.

15. Deng Q, Yin X, Wang D, Abdel Wahab M. Numerical analysis of crack propagation in fretting fatigue specimen repaired by stop hole method. Int J Fatigue. 2022;156:106640. doi:10.1016/j.ijfatigue.2021.106640.
16. Fang L, Fu Z, Ji B, Fan J. Reinforcement effect of high-strength bolts for stop-hole under out-of-plane bending loads. J Bridge Eng. 2023;28(1):04022129. doi:10.1061/jbenf2.beeng-5711.
17. Gong H, Jin Z-G, Yang F-P, Mao W-T. Analysis of stop-hole effects on mode I-II fatigue crack behavior for Q420 steel using experiments, FEM and variable length RNN approaches. Theor Appl Fract Mech. 2023;124:103823. doi:10.1016/j.tafmec.2023.103823.
18. Anoop Kumar A, Arunkumar S, Arutselvan CK, John J. Analysis of stress intensity factor of a finite plate with centre crack containing different hole shapes. Mater Today Proc. 2023;80:790–8. doi:10.1016/j.matpr.2022.11.130.
19. Neto DM, Cavaleiro N, Sérgio ER, Jesus J, Camacho-Reyes A, Antunes FV. Effect of crack flank holes on fatigue crack growth. Int J Fatigue. 2023;170:107505. doi:10.1016/j.ijfatigue.2023.107505.
20. Baptista R, Moita P, Infante V. Fatigue crack growth on modified CT specimens using artificial neural networks. Int J Fatigue. 2023;167:107357. doi:10.1016/j.ijfatigue.2022.107357.
21. Liu Z, Li Z, Huang C, Jiang X. An investigation on the fatigue performance of cracked steel plates reinforced with FRP and stop hole. Mech Adv Mater Struct. 2022;29(25):3646–57. doi:10.1080/15376494.2021.1907005.
22. Feng L, Ling L, Meng C, Ji B. Analysis on stop-hole parameters for fatigue cracks at Arc Notch in steel bridge deck. J Phys Conf Ser. 2022;2148(1):012036. doi:10.1088/1742-6596/2148/1/012036.
23. Parsania A, Kakavand E, Hosseini SA, Parsania A. Estimation of multiple cracks interaction and its effect on stress intensity factors under mixed load by artificial neural networks. Theor Appl Fract Mech. 2024;131:104340. doi:10.1016/j.tafmec.2024.104340.
24. Zhang L, Wei X. Prediction of fatigue crack growth under variable amplitude loading by artificial neural network-based Lagrange interpolation. Mech Mater. 2022;171:104309. doi:10.1016/j.mechmat.2022.104309.
25. Paris P, Erdogan F. A critical analysis of crack propagation laws. J Basic Eng. 1963;85(4):528–5. doi:10.1115/1.3656900.